

Inhibition of TRPM3 by Primidone Provides a Potential Therapeutic Method for Adenomyosis Management

Zhixing Jin^{1,*}, Yaoming Peng^{2,*}, He Zhang¹, Xiaoping He², Yi Zhang¹, Xin Pan¹, Min Li¹, Qianqian Yang³

¹Department of Obstetrics and Gynecology, The First Affiliated Hospital of Soochow University, Suzhou, Jiangsu, 215123, People's Republic of China;

²Shanghai Obstetrics and Gynecology Hospital, Fudan University, Shanghai, 200011, People's Republic of China; ³Department of Pathology, the First Affiliated Hospital of Soochow University, Suzhou, Jiangsu, 215123, People's Republic of China

*These authors contributed equally to this work

Correspondence: Min Li, Department of Obstetrics and Gynecology, The First Affiliated Hospital of Soochow University, 899 Pinghai Road, Suzhou, Jiangsu, 215123, People's Republic of China, Email 18321706891@163.com; Qianqian Yang, Department of Pathology, The First Affiliated Hospital of Soochow University, 899 Pinghai Road, Suzhou, 215123, Jiangsu, People's Republic of China, Email qianqianyang2023@163.com

Purpose: To test the expression profile of transient receptor potential channels (TRPs) in adenomyosis patients and evaluate the effects of primidone on tamoxifen-induced adenomyosis mice.

Patients and Methods: This study included in vivo animal model and human tissue samples. Eutopic endometrium from adenomyosis patients (n=20) was collected and subjected to mRNA analysis of TRP channels. TRPA1, TRPV1 and TRPM3 in adenomyosis patients (n=50) and tamoxifen-induced adenomyosis mice (n=6) were examined by immunohistochemistry. From 10 weeks after birth, primidone (2 mg/kg/d) and atosiban (1 mg/kg/d) were given separately to adenomyotic mice by intraperitoneal injection for 3 weeks. The hotplate test was conducted once a week beginning at 10 weeks, and then uterine samples were harvested for HE staining and RNA-seq at 13 weeks.

Results: The mRNA expression of 15 TRPs was significantly increased in the proliferative phase of the adenomyotic endometrium. TRPV1, TRPM3 or TRPA1 staining levels were positively correlated with dysmenorrhea severity, menses amount and uterine size. In tamoxifen-induced adenomyosis mice, primidone had a significant effect on both the depth of myometrial infiltration and analgesia. Forty-seven DEGSSs were identified after primidone treatment, and bioinformatics analysis predicted that they were enriched in the cell cycle and cell division.

Conclusion: The expression profile of TRP channels varies significantly in adenomyosis patients, and primidone may provide a potential therapeutic method for adenomyosis management.

Keywords: adenomyosis, TRPs, primidone, pelvic pain, TRPM3

Introduction

Adenomyosis (AMS) is a common gynecologic disorder in which endometrial glands and stroma are found within the myometrium with a range of symptoms, such as progressive dysmenorrhea, menorrhagia and infertility, which affect the quality of life of 20 to 35% of women of reproductive age and consume substantial health care resources.¹ Among all complaints from women with adenomyosis, dysmenorrhea and other types of pain, including cyclic or acyclic lower abdominal pain, cyclic dysuria and dyspareunia, are the most common and are the most debilitating.² Treatment of adenomyosis typically starts with hormonal menstrual suppression. Patients with adenomyosis may ultimately undergo a hysterectomy if symptoms are not controlled with medical therapy.³ The choice depends on the woman's age, reproductive status, and clinical symptoms. Nonetheless, the disease is increasingly diagnosed in young women with reproductive desires, and thus conservative treatments should be preferred. However, symptom recurrence after drug

discontinuation, obvious side effects and pregnancy limitations are the principal drawbacks of the use of suppressive hormones.⁴ Although nonsteroidal anti-inflammatory drugs (NSAIDs) can alleviate menstrual pain, approximately 18% of women with dysmenorrhea are unresponsive to these drugs, which caused these patients and their physicians to pursue less well-studied strategies.⁵

One attractive approach is to target the very beginning of the pain pathway, focusing on nociceptive receptors.⁶ Transient receptor potential (TRP) channels play central receptors in the transduction of nociceptive stimuli by altering the membrane potential or intracellular calcium concentration. In mammals, the TRP superfamily includes TRP vanilloid (TRPV), TRP ankyrin (TRPA), TRP melastatin (TRPM), and TRP canonical (TRPC) channels, which can be activated by a variety of stimuli and are widely distributed throughout the body.⁷ In normal endometrial biopsies, TRP channel expression has been shown to fluctuate during the menstrual cycle and is regulated by the female hormones estradiol and progesterone,⁸ among which TRPV1, TRPM3 and TRPA1 are of particular interest.⁹ Nonetheless, the inhibition of pain by overwhelming TRPV1 and TRPA1 was largely halted because of hyperthermia, which could put patients at risk for scalding injuries by elevating the heat pain threshold.¹⁰ In this respect, TRPM3 has gained popularity as the latest TRP family member to study.¹¹

However, current knowledge about the distribution of TRP channels in adenomyosis is scarce. To identify members of the TRP superfamily involved in adenomyosis, RNA and protein expression studies were performed on tissue obtained during endometrial biopsies from adenomyosis patients during different phases of the menstrual cycle and their correlation with the severity of dysmenorrhea was revealed. In addition, the TRPM3 antagonist primidone and the antagonist of the oxytocin receptor atosiban were used for the first time in a mouse model of tamoxifen-induced adenomyosis, which may provide a potential therapeutic method for adenomyosis management.

Materials and Methods

Ethics Statement

This study complied with the tenets of the Declaration of Helsinki and the National Guidelines for Animal Use in Research (China). All experiments were performed under the guidelines of the National Research Council Guide for the Care and Use of Laboratory Animals. This study protocol was reviewed and approved by the Medical Ethics Committee of the First Affiliated Hospital of Soochow University (Suzhou, China), approval number 2020–149 and the Institutional Ethics Review Board of the Shanghai Obstetrics and Gynecology Hospital (Shanghai, China), approval number 2020–27. All tissue samples were obtained after written, full and informed consent was obtained from the enrolled subjects.

Patients and Human Tissue Collection

All the samples used in this study were collected at the First Affiliated Hospital of Soochow University (Suzhou, China) and the Shanghai Obstetrics and Gynecology Hospital (Shanghai, China) from June 2021 to June 2022. To reveal the expression profile of TRP channels in endometrial biopsies using RT–PCR analysis, twelve patients without adenomyosis (proliferation phase $n=6$; secretory phase $n=6$) and twenty patients with adenomyosis (proliferation phase $n=13$; secretory phase $n=7$) were enrolled at different times during menstruation. For further protein examination by immunohistochemistry, fifty human endometrial samples from adenomyosis patients (proliferation phase $n=29$; secretory phase $n=21$) and twenty-one control subjects (proliferation phase $n=14$; secretory phase $n=7$) were collected. The diagnosis of adenomyosis was made by transvaginal ultrasound before surgery then histologically confirmed postoperatively, who only had adenomyosis and were free of endometriosis, uterine fibroids, infertility and other gynecological or reproductive disorders. For controls, endometrial tissue samples were collected from women who had undergone hysterectomy because of cervical intraepithelial neoplasia (CIN)-III, cervical carcinoma in situ and stage IA1 cervical cancer but were free of endometriosis, adenomyosis, uterine fibroids, infertility and other gynecological or reproductive disorders. All the recruited women in both the adenomyosis and control groups had not received any hormonal or antiplatelet treatment for at least 3 months prior to tissue collection. Two wedges of tissue from the lumen to the muscular myometrial layer that included superficial and basal endometrium as well as myometrium were taken from the detached uterus. One was immediately fixed in 10% neutral-buffered formalin at room temperature for 48 h and then embedded in

paraffin for hematoxylin and eosin (HE) or immunohistochemical staining, and the other was stored in liquid nitrogen for RNA extraction. Information on uterine size, severity of dysmenorrhea, menstrual volume, cycle length, reproductive history and age was also recorded. Uterine size is measured via ultrasound and calculated by length*width*height. Depending on whether they changed their sanitary pads <3, between 3 and 6 or >6 times a day, respectively, their amount of menses during menstruation was grouped into three classes: light, moderate and heavy. The severity of dysmenorrhea was classified as none, mild (pain but no interference with routine daily life or work and no need for analgesics), moderate (pain interfering with routine daily life or work to some extent and relief of pain after taking analgesics), and severe (pain seriously interfering routine daily life or work and no relief of pain after taking analgesics).¹²

Real-Time Polymerase Chain Reaction (RT-PCR)

Total RNA was isolated from endometrial tissues via a DNA/RNA/Protein isolation kit (Tiangen, China), and 1 µg of the purified total RNA was reverse transcribed into cDNA using a PrimeScript RT Master Mix kit (Takara, Japan) according to the manufacturer's protocol. RT-PCR was performed with the CFX96 real-time PCR detection system (Bio-Rad, USA) and a TB Green Premix Ex Taq II kit (Takara, Japan). The primers used in the experiment are shown in Table 1. The relative expression of each gene was calculated using the delta-delta Ct method, with GAPDH serving as the endogenous control.

Immunohistochemistry (IHC)

Each paraffin-embedded tissue block was subjected to serial 3 mm sectioning for immunohistochemical staining of TRPV1 (1:200; Alomone, Israel), TRPA1 (1:200; Alomone, Israel), TRPM3 (1:200; Alomone, Israel) and α -SMA

Table 1 Primer Sequences

| Gene | Species | Sense Primer | Antisense Primer |
|---------|---------|------------------------|-------------------------|
| TRPV1 | Human | GTGCCGTTTCATGTTTGTCTA | AGTCATTCTTCCCGTCTTCAA |
| TRPV2 | Human | ATCTGCTCATCCCCAAGTTCT | GCTTCTTCAGGGTAGGCTGAT |
| TRPV3 | Human | TTCTATTTGCCTAACCTGCCA | AATTCCATCCAGACCCACAG |
| TRPV4 | Human | CCGTCTCCTTCTACATCAACG | GGTAGTAGGCGGTGAGAGTGA |
| TRPV5 | Human | GATCAGAATCCTCTGCGAGTG | TTTCTCAGATGGATGCTCCTG |
| TRPV6 | Human | TTCCTGGAAGTTGCTCTCATT | GCGTTCATGCTACTCCTCTTT |
| TRPM1 | Human | GCATAAAGAGCAGTTTGCAGA | TCCATCCCATTCTGTCACTA |
| TRPM2 | Human | CTTCTGGTTTGGTGTCAACAG | GGCAGATTTAATGTCTTGGGT |
| TRPM3 | Human | TCCTCTTACACCTGATGACCA | GCTTTGATGAGCCCTTTCC |
| TRPM4 | Human | CACTGTCTCTGCATCGACT | GCTGTTTGTGACCGTGAAG |
| TRPM5 | Human | TTGCTGCCCTAGTGAACCA | TGTCCTCCCAAGAGAAATGCT |
| TRPM6 | Human | GAGACCATGCTGGGATAGATT | GTATCTGTTGGGCTTTTCGTT |
| TRPM7 | Human | CCTCAGTTGCGAAAGAGTCAT | GGTAGGGCTGTGCTGTCTTAAT |
| TRPM8 | Human | AGGCAACCTCTAGCGATTACC | CACAAAGATGCTCATCCCAAT |
| TRPC1 | Human | CGTTACCTCCACCTTTCAACAT | CTGTTTTGCCGTTTGACCTT |
| TRPC3 | Human | GCCGAGACTCAGAAGAGGTAGA | TTAATGGCAAGTTTGACACGAC |
| TRPC4 | Human | CCAGACACAGTCACCCACGAAG | TTCCCCCAGAGCACTAC |
| TRPC5 | Human | AGACATCTCCAGCTTTCGGTA | CCACTGCCATCATTATTATCGT |
| TRPC6 | Human | TGATCGCTCCACAAGCCTATCT | CCGCACCACTGGGATGTTAC |
| TRPC7 | Human | CTGGCAGACCTGATTCAACAA | GTAGAAGTCACAGACGCCGATG |
| TRPA1 | Human | AGGGAGCCACTGAGATTGTT | ATGACATCCATCGTTGTGT |
| CHIL1 | Mouse | TTACAGGATTGAGGGACCATAC | AAAGGGAAGTGGGACGATTA |
| COL9A2 | Mouse | TGAGGCTTCTGGTGGTCCTTAC | TCTCCCCAAAAGATACCCAAT |
| PSMC3IP | Mouse | TGGAGGTGGGAACAGAGCGT | ACACTATGGCTTTGTGCTCCGTC |
| NEIL3 | Mouse | GGAGAGGATTGCTTTACGGACT | TTAGCCGAGGGTCTGTTTATGAG |
| SPC24 | Mouse | GGAGCCAGAGCCTTGACCT | CAATGAACGCACTCACATACAGA |
| GAPDH | Human | GGGAAGGTGAAGTCCGAGT | GGGGTCATTGATGGCAACA |
| GAPDH | Mouse | ACCCAGAAGACTGTGGATGG | CACATTGGGGGTAGGAACAC |

(1:200; Abcam, USA). The quantification of immunoreactivity was performed with Image-Pro Plus 6.0 software (Media Cybernetics Inc., USA). Briefly, paraffin-embedded slides were deparaffinized, rehydrated and washed in PBS (pH 7.4) three times for 15 min each time. Then, the sections were subjected to antigen retrieval with citric acid buffer (pH 6.0) at 98 °C for 30 min. Next, they were treated with 3% hydrogen peroxide (Beyotime Institute of Biotechnology), blocked with 10% goat serum (Beyotime Institute of Biotechnology) for 1 h at room temperature and incubated with the aforementioned primary antibodies or PBS (negative control) overnight at 4 °C. After three washes in PBS (pH 7.4) for 15 min each time, the sections were incubated with a horseradish peroxidase-conjugated secondary antibody (cat. no. ab6728; 1:2,000; Abcam) at room temperature for 60 min. Subsequently, the sections were washed again in PBS and incubated with 0.01% 3,3'-diaminobenzidine tetrahydrochloride (Beyotime Institute of Biotechnology) for 2 min at room temperature. The sections were then washed thoroughly in PBS three times for 5 min each time, stained with hematoxylin for 20 sec at room temperature, dehydrated in an ascending absolute alcohol gradient, placed in xylene and mounted in synthetic resin for light microscopic examination. The quantification of immunoreactivity was determined with Image-Pro Plus 6.0 software (Media Cybernetics Inc., USA), as previously described.¹³

Preparation of Drugs & Animals and Animal Specimen Collection

Administering tamoxifen orally to Institute of Cancer Research (ICR) newborn mice is a classic method to establish an experimental adenomyosis model. Tamoxifen was purchased from MedChemExpress Company (HY-13757A, New Jersey, USA). A total of thirteen 19-day pregnant ICR mice weighing 40–50 g were purchased from the Laboratory Animal Center of the Shanghai Institutes of Biological Sciences (Shanghai, China). Each dam and her pups were housed in the same cage under controlled conditions (12:12 light/dark cycle, 70–80% humidity, 22–24 °C) and had access to chow and fresh water ad libitum.

Before drug administration, we used 25 female neonatal mice from among the 7 pregnant ICR mice to calculate the rate of adenomyosis formation by HE staining by being euthanized using 5% isoflurane for 5 mins followed by cervical dislocation separately at Day 5, Day 10, Day 15, Day 25 and Day 42. For primidone and atosiban treatment, we obtained 24 female neonatal mice from 6 pregnant ICR mice, while in total of fifty-three male neonatal progeny were euthanized using 5% isoflurane for 5 mins followed by cervical dislocation, and the death was confirmed by a lack of heartbeat and respiration. The female neonates were randomly divided into four groups: i) control (n=6); ii) ADE model (n=6); iii) primidone (n=6; Sigma, USA); and iv) atosiban (n=6; Sigma, USA). From Day 1 to Day 5 after birth, female neonatal mice in the ADE group and drug treatment groups received 1 mg/kg tamoxifen suspended in a peanut oil/lecithin/condensed milk mixture (2:0.2:3, by volume) at a dose volume of 5 µL/g body weight, while the control neonatal mice were fed similarly with the same amount of solvent without tamoxifen. All mice were weaned and separated from the dams upon reaching 3 weeks of age. The thirteen adult ICR mice at the end of the experiment were euthanized via inhalation of 5% isoflurane for 5 min followed by cervical dislocation, and death was confirmed by a lack of heartbeat and respiration.

From ten weeks after birth, mice in the drug treatment groups were administered with either primidone (2 mg/kg/d) or atosiban (1 mg/kg/d) daily via intraperitoneal injection for 3 weeks, whereas the mice in the control and ADE groups were administered similarly with corresponding quantities of the vehicle. All the mice were subjected to a hotplate test once a week for 3 weeks beginning at 10 weeks of age. All the mice had a normal estrus cycle. The mice were euthanized using 5% isoflurane for 5 mins followed by cervical dislocation and uterine samples from the mice in the four aforementioned groups were harvested at 13 weeks of age after the last hotplate test. Then the uteri were then excised, where half of the samples were immediately fixed in 4% paraformaldehyde at room temperature for 48 h and all remaining uterine tissue samples were placed immediately in liquid nitrogen for subsequent mRNA array. Humane endpoints during the experiment were defined as food-water intake difficulties, weight loss $\geq 20\%$ of the body weight, and reduced activities and movement.

Hotplate Test Procedure

As described previously,⁴ a commercially available Hot Plate Analgesia Meter (BME-480; Chinese Academy of Medical Sciences, China) was used for the hotplate test. The surface of the plate was heated to and maintained at a constant temperature of 50.0 \pm 0.1°C as measured via a built-in digital thermometer. A plastic cylinder 20 cm in diameter and

18 cm in height was placed on the hotplate. All the mice were allowed to acclimatize under a controlled environment at 22–24°C with 70–80% humidity in the testing room for 10 min prior to test commencement. The latency response to thermal stimuli was defined as the time (sec) elapsed from the moment the mouse was placed inside the cylinder to the moment it licked its hind paws. Each mouse was tested once per session. The latency was calculated as the mean between two readings recorded between 24 h intervals.

RNA Sequencing (RNA-Seq) and Data Analysis

RNA-seq and analysis were conducted by OE Biotech Co. (Shanghai, China). Briefly, after collecting uterus tissues from mice in different groups, total RNA was extracted and quantified with a NanoDrop 2000 spectrophotometer (Thermo Fisher Scientific, USA). RNA quality was assessed using the Agilent 2100 Bioanalyzer (Agilent Technologies, Santa Clara, CA, USA), and RNA samples with RIN >7.0 were subjected to further processing.

Then, the libraries were constructed using the TruSeq Stranded mRNA LT Sample Prep Kit (Illumina, USA) and subsequently sequenced on an Illumina NovaSeq 6000 platform and 150 bp paired-end reads were generated. Raw reads of fastq format were firstly processed using fastp and the low quality reads were removed to obtain the clean reads. Then about 6.71~7.34 G clean reads for each sample were retained for subsequent analyses. The clean reads were mapped to the reference genome using HISAT2 (<https://ccb.jhu.edu/software/hisat2/index.shtml>). Gene expression was calculated using FPKM (Fragments Per kb Per Million Reads), which is the number of fragments per kilobase length of a protein-coding gene per million fragments. Raw reads of fastq format were firstly processed using fastp (Version 0.20.1) and the low quality reads were removed to obtain the clean reads, where the parameter used is length required 50, and the read counts of each gene were obtained by HTSeq-count. PCA analysis was performed using R (v 3.2.0) to evaluate the biological duplication of samples.

Differentially expressed genes (DEGs) between the two groups were identified using the DESeq R package (R Foundation for Statistical Computing; <http://www.r-project.org/>). The threshold was set as false discovery rate-adjusted P value <0.05 and fold change >2 or fold change <0.5. DEGs that were increased/decreased in adenomyosis mice and then decreased/increased after primidone treatment were identified. Hierarchical cluster analysis of these DEGs was performed to demonstrate the expression pattern of genes in different groups. Based on the hypergeometric distribution, GO and KEGG pathway enrichment analyses of these selected DEGs were further performed to screen the significantly enriched terms using R. The raw RNA-seq data were deposited in the Gene Expression Omnibus database (available: <https://www.ncbi.nlm.nih.gov/geo>; accession number GSE227384).

Statistical Analysis

Statistical differences were analyzed using the Statistical Package for the Social Sciences (SPSS) software (22.0) (Chicago, USA). Two-tailed unpaired Student's *t* test, one-way ANOVA followed by Tukey's multiple comparisons test, the Kruskal–Wallis test followed by Dunn's multiple comparison test, and Pearson's and Spearman correlation analysis were used for further analyses. P values of 0.05 were considered statistically significant.

Results

mRNA Expression Profile of TRP Channels in Eutopic Endometrial Biopsies from Patients with and without Adenomyosis Throughout the Menstrual Cycle

The characteristics of the recruited patients with adenomyosis and the control subjects with respect to the mRNA expression profile of TRP channels in the eutopic endometrium are listed in Table 2. As shown in the table, the patients in the different groups were comparable in age, live births, miscarriages and cycle length. However, patients with adenomyosis have significantly larger uterine sizes, heavier menses and more severe dysmenorrhea.

RT–PCR analysis was used to investigate the expression profiles of TRP channels in endometrial biopsies from control (proliferation phase n=6; secretory phase n=6) and adenomyosis (proliferation phase n=13; secretory phase n=7) patients harvested at different times during menstruation (Figure 1A). Compared with proliferative endometrium of control patients, the mRNA expression levels of TRPM1, TRPM3, TRPM4, TRPM6, TRPM7, TRPM8, TRPC1, TRPC3,

Table 2 Characteristics of Recruited Patients with and without Adenomyosis for mRNA Expression Profile of TRP Channels in Endometrial Biopsies

| Variable Name | Control Proliferative Phase n=6 | Control Secretory Phase n=6 | Adenomyosis Proliferative Phase n=13 | Adenomyosis Secretory Phase n=7 | p-value |
|--|--|--|---|---|---------|
| Age (years) Median (range) Mean (\pm S.D.) | 38(36–47) 40.0 \pm 4.8 | 41(31–51) 40.5 \pm 8.0 | 47(36–54) 45.9 \pm 4.7 | 46(38–54) 46.0 \pm 5.5 | 0.09 |
| Live births Median (range) | 1(1–2) | 1.5(1–2) | 1(1–2) | 1(1–2) | 0.32 |
| Miscarriage Median (range) | 1(0–2) | 1(0–2) | 1(0–2) | 1(0–1) | 0.88 |
| Cycle length (days) Median (range) | 27(25–30) | 30(30–30) | 30(26–33) | 28(23–30) | 0.06 |
| Menstrual volume Light & Moderate Heavy | 5(83.3%) 1(16.7%) | 6(100%) 0(0%) | 7(53.8%) 6(46.2%) | 0(0%) 7(100%) | <0.0001 |
| Severity of dysmenorrhea None Mild Moderate Severe | 4(66.7%) 2(33.3%) 0(0%) 0(0%) | 4(66.7%) 2(33.3%) 0(0%) 0(0%) | 2(15.4%) 1(7.7%) 6(46.2%) 4(30.7%) | 0(0%) 1(14.2%) 3(42.9%) 3(42.9%) | <0.0001 |
| Uterine size (in cm3) Mean (\pm S.D.) | 117.0 \pm 30.12 | 152.7 \pm 56.82 | 531.0 \pm 312.6 | 521.1 \pm 324.6 | 0.0029 |

TRPC4, TRPC5, TRPC6, TRPV4, TRPV5, and TRPA1 were significantly increased during the secretory phase of control patients (Figure 1B–D). Moreover, we compared the endometrium during the proliferation phase in controls with that during the same phase in adenomyosis patients and found that with the exception of TRPV4, TRPC7, TRPM2, TRPM4, TRPM5, and TRPM8, the mRNA expression of the other 15 TRP channels was significantly elevated in adenomyosis. No significant difference was found when the secretory phase of the control endometrium was compared with the same phase of the adenomyosis endometrium. Taken together, these results illustrate a distinct TRP channel expression pattern between the endometrium in control patients and the endometrium in adenomyosis patients.

The Expression of TRPV1, TRPM3 and TRPA1 in the Endometrium of Adenomyosis Patients by IHC

The characteristics of the recruited patients with adenomyosis (proliferation phase n=29; secretory phase n=21) and the control subjects (proliferation phase n=14; secretory phase n=7) with respect to the expression of TRPV1, TRPM3 and TRPA1 in the endometrium are listed in Table 3. Immunohistochemistry was performed to determine the expression of TRPV1, TRPM3 and TRPA1 at the protein level. TRPV1 and TRPA1 staining was mainly observed in endometrial epithelial cells in both control and adenomyosis tissues and was mostly localized in the cytomembrane. TRPM3 staining was observed in both epithelial and stromal cells and was localized in the cytoplasm and cytomembrane (Figure 2A).

In the control endometrium, the staining levels of TRPM3, TRPV1 and TRPA1 were not significantly different at various times during menstruation. Consistent with previous results at the mRNA level, TRPM3 and TRPA1 proteins were highly expressed in the endometrium during the proliferation phase in adenomyosis patients compared with the same phase of the endometrium in the control patients (Figure 2B and C). Moreover, the expression of TRPV1 was markedly greater in the

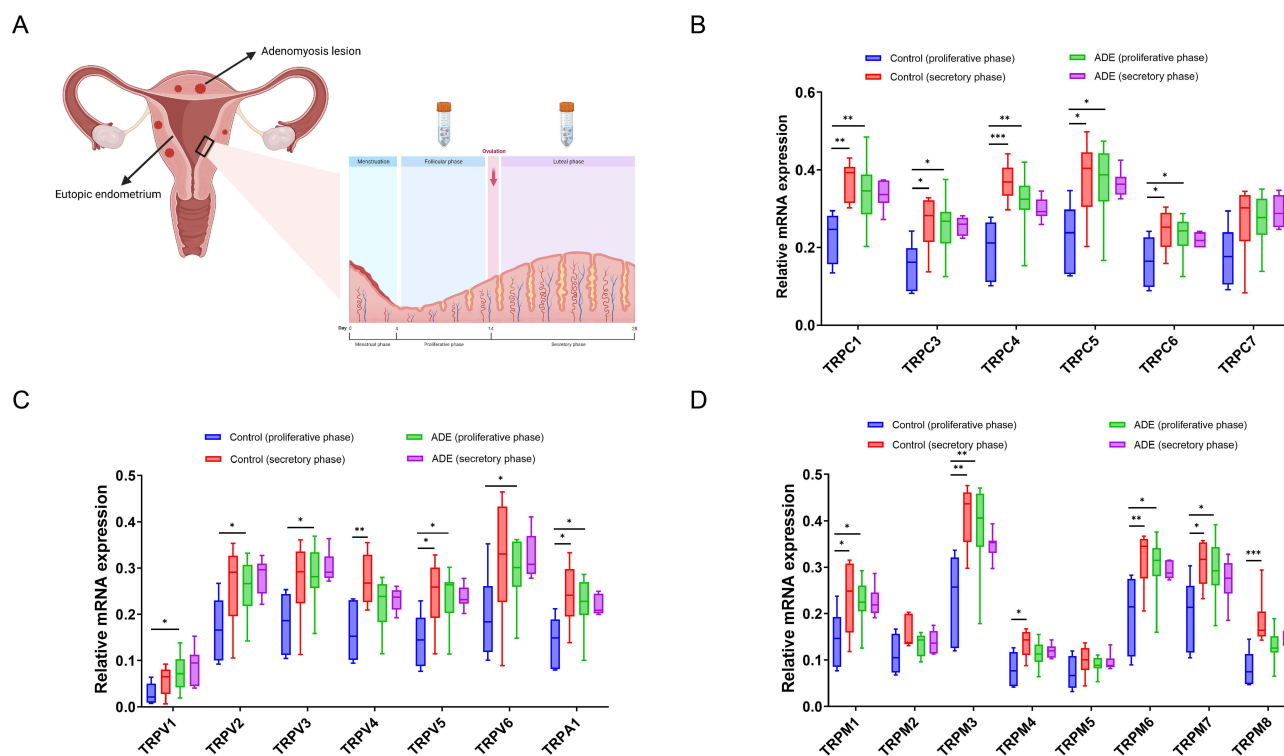


Figure 1 mRNA expression levels of TRP channels in eutopic endometrium throughout the menstrual cycle. **(A)** The scheme of adenomyosis as indicated in a cartoon and the menstrual cycle is displayed to show which days of the cycle are included for sample collection in the different cycle phases, which was generated using BioRender.com. **(B–D)** mRNA levels of members of the TRPV(**B**), TRPC(**C**) and TRPM(**D**) subfamilies respectively in the eutopic endometrium of subjects with or without ADE; the levels are relative to the geometric mean of housekeeping gene GAPDH, during the proliferation phase or secretory phase. Significant differences in RNA expression during the different phases of the menstrual cycle were assessed via one-way ANOVA test followed by Tukey's multiple comparisons test. Symbols for statistical significance levels: * $P < 0.05$, ** $P < 0.01$ and *** $P < 0.001$.

secretory phase of the endometrium of adenomyosis patients than in the same phase of the endometrium in the control patients; however, no obvious changes were observed in the endometrium in the proliferative phase (Figure 2D).

The Severity of Dysmenorrhea Was Positively Correlated with TRPV1, TRPM3 or TRPA1 Staining Levels

Since dysmenorrhea is one of the major complaints in women with adenomyosis, we used immunohistochemistry to examine whether TRPV1, TRPM3 and TRPA1 are associated with the severity of dysmenorrhea in women with adenomyosis. We found that the TRPV1, TRPM3 and TRPA1 staining levels were significantly correlated with the

Table 3 Characteristics of Recruited Patients With and Without Adenomyosis for the Expression of TRPV1, TRPM3 and TRPA1 in Endometrium at Protein Level

| Variable Name | Control Proliferative Phase n=14 | Control Secretory phase n=7 | Adenomyosis Proliferative Phase n=29 | Adenomyosis Secretory Phase n=21 | p-value |
|--------------------|----------------------------------|-----------------------------|--------------------------------------|----------------------------------|---------|
| Age (years) | | | | | |
| Median (range) | 41.5(36–52) | 42(39–51) | 47(37–52) | 45(34–53) | |
| Mean (\pm S.D.) | 42.4 \pm 5.5 | 44.6 \pm 5.1 | 45.6 \pm 4.9 | 44.3 \pm 4.8 | 0.21 |
| Live births | | | | | |
| Median (range) | 1(0–3) | 1(1–2) | 1(0–3) | 1(0–2) | 0.71 |

(Continued)

Table 3 (Continued).

| Variable Name | Control Proliferative Phase n=14 | Control Secretory phase n=7 | Adenomyosis Proliferative Phase n=29 | Adenomyosis Secretory Phase n=21 | p-value |
|---|---|--|---|---|---------|
| Miscarriage Median (range) | 1(0–2) | 1(0–2) | 1(0–2) | 1(0–1) | 0.37 |
| Cycle length (days) Median (range) | 28(25–30) | 30(28–30) | 30(23–40) | 30(23–35) | 0.13 |
| Menstrual volume Light & Moderate Heavy | 13(92.9%) 1(7.1%) | 7(1000%) 0(0%) | 14(48.3%) 15(51.7%) | 7(33.4%) 14(66.6%) | <0.0001 |
| Dysmenorrhea severity None Mild Moderate Severe | 12(85.7%) 2(14.3%) 0(0%) 0(0%) | 5(71.4%) 2(28.6%) 0(0%) 0(0%) | 4(13.8%) 4(13.8%) 13(44.8%) 8(27.6%) | 1(4.8%) 2(9.5%) 5(23.8%) 13(61.9%) | <0.0001 |
| Uterine size (in cm3) Mean (±S.D.) | 108.6±34.85 | 173.7±76.10 | 650.1±560.6 | 628.9±288.8 | 0.0001 |

severity of dysmenorrhea, and TRPM3 showed the strongest correlation. (Spearman's $r=0.3234/P=0.0141$, $r=0.5688/P<0.0001$ and $r=0.3657/P=0.0044$, respectively; [Figure 3A-C](#)).

Menstrual Volume and Determination of TRPV1, TRPM3 or TRPA1 Immunoreactivity

We next examined the relationships, if any, between TRPV1, TRPM3 or TRPA1 immunoreactivity and the menstrual volume. Since there was only one woman who reported light menses, we divided all cases into two groups: women who reported light or moderate menses and those who reported heavy menses. We found that higher TRPV1, TRPM3 or TRPA1 staining in the eutopic endometrium was easier to observe in women with heavy menses, but their associations were weak. (Spearman's $r=0.3117/P=0.018$, $r=0.3158/P=0.0158$, $r=0.3846/P=0.0026$, respectively; [Figure 3D-F](#)).

Uterus Size and TRPV1, TRPM3 or TRPA1 Immunoreactivity

As an enlarged uterus is one of three major presentations of adenomyosis after abnormal uterine bleeding and dysmenorrhea, we also examined the relationship between uterus size and TRPV1, TRPM3 or TRPA1 immunoreactivity. We found that larger uterus sizes were more frequently observed in those with higher expression of TRPV1, TRPM3 or TRPA1 in the endometrium, and TRPA1 showed the strongest correlation. (Pearson's $r=0.3182/P=0.0190$, $r=0.3001/P=0.0246$ and $r=0.3914/P=0.0029$, respectively; [Figure 3G-I](#)).

TRPV1, TRPM3 and TRPA1 Expression Was Upregulated in Mice With Tamoxifen-Induced Adenomyosis

To determine whether mouse endometrial epithelial cells or stromal cells have a transient receptor potential (TRP) channel expression profile similar to that found in the human endometrium, tamoxifen was used to induce adenomyosis in newborn ICR mice.

Mice in each group were killed at Day 5, Day 10, Day 15, Day 25 and Day 42 to calculate the rate of adenomyosis formation by HE staining. The presence of any ectopic endometrium in the myometrium was considered a successful establishment of the adenomyosis mouse model. On Day 42, all mice in the adenomyosis model group exhibited endometrial invasion into the myometrium, whereas no ectopic endometrium was observed in the myometrium of the control group

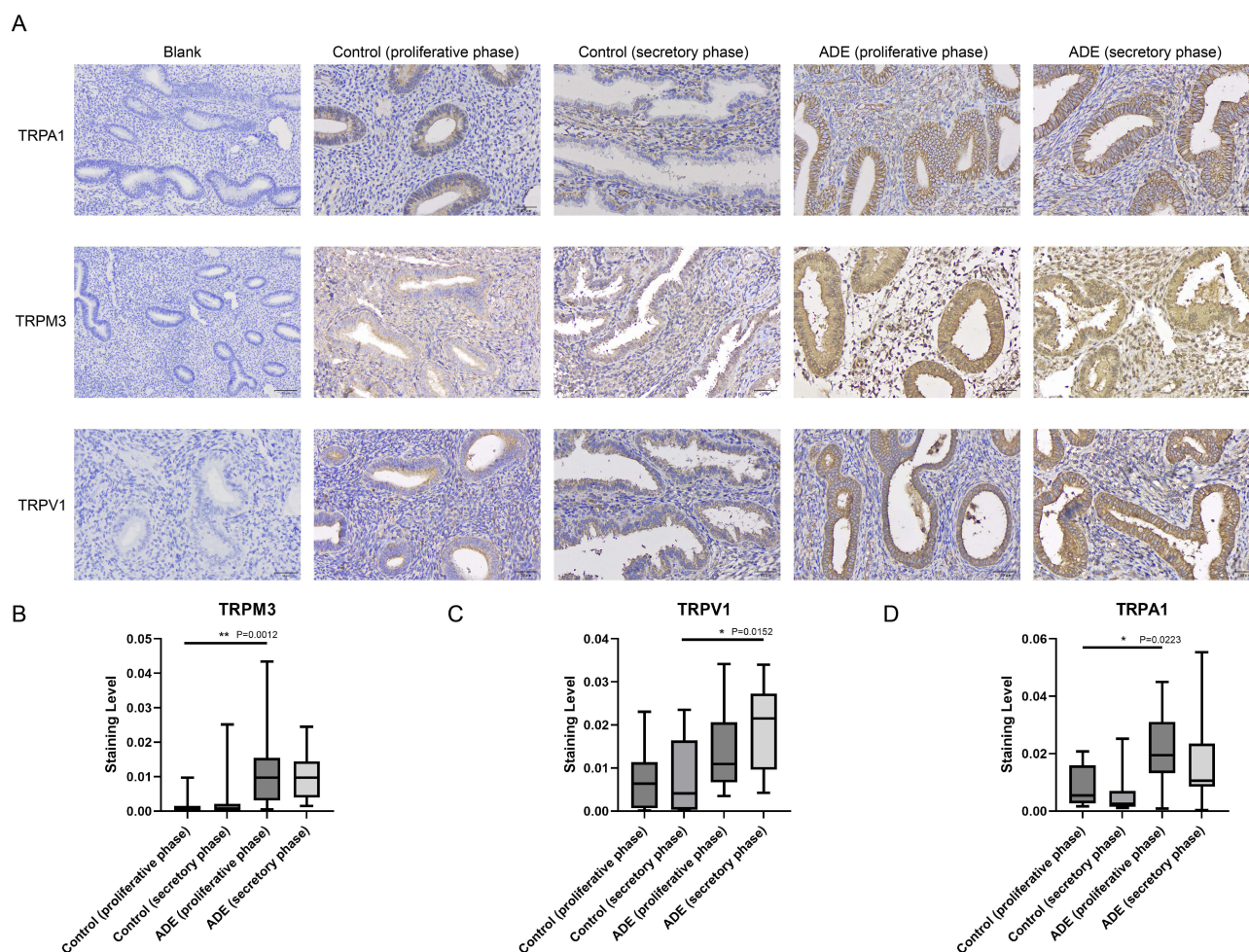


Figure 2 Protein expression of TRPV1, TRPM3 and TRPA1 in the eutopic endometrium of adenomyosis patients. **(A)** Representative images of TRPV1, TRPM3 and TRPA1 in patients with or without ADE during different phases of menstruation. Scale bars, 50µm. **(B-D)** Quantitative analysis of TRPA1 **(B)**, TRPM3 **(C)**, and TRPV1 **(D)** expression in patients with or without adenomyosis throughout the menstrual cycle. Significant differences in RNA expression during the different phases of the menstrual cycle were assessed with the Kruskal–Wallis test for non-parametric data followed by Dunn’s multiple comparison test. Symbols for statistical significance levels: *P < 0.05 and **P < 0.01.

(Figure 4A). Compared with those in the control group, the expression levels of TRPV1, TRPM3 and TRPA1 was significantly increased, and their expression position and levels were similar to those in human samples (Figure 4B-C).

The Effects of TRPM3 Inhibitor Primidone and Oxytocin Receptor Antagonist Atosiban on Hot Plate Response Latency Following Adenomyosis Establishment

The hotplate test is a commonly used method for measuring nociception and evaluating response thresholds to thermal stimuli in rodents. In the present study, all mice were subjected to hot plate testing once per week beginning at 10 weeks after birth. At 13 weeks, the mice in different groups were sacrificed after being weighed and subjected to the hotplate test (Figure 5A). We found no significant difference in body weight among the groups (Figure 5B). Compared with that in mice from the control group, the hot plate response latency in mice from the ADE group was significantly decreased. After 2 weeks of treatment with primidone and 3 weeks of treatment with atosiban, a significantly prolonged response latency was observed in both treatment groups compared with the ADE group, and primidone exhibited a better analgesic effect than atosiban (Figure 5C).

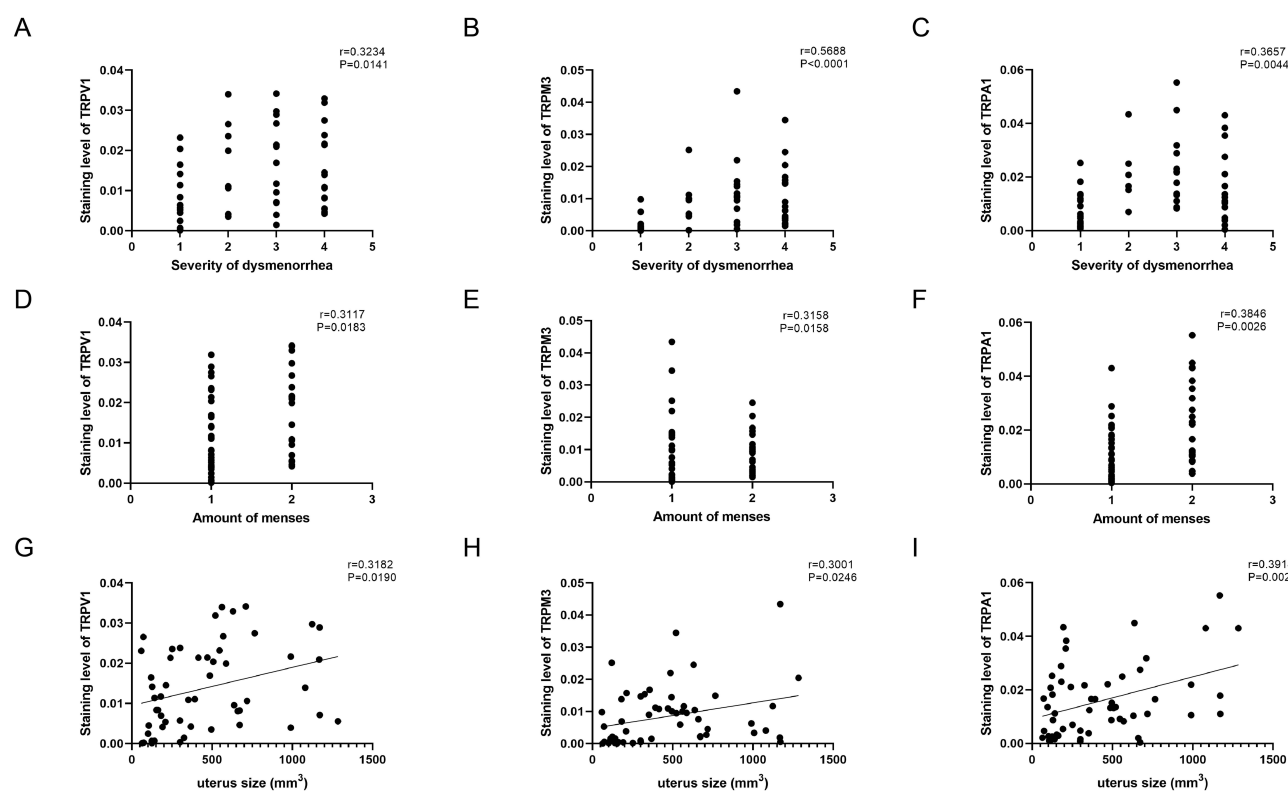


Figure 3 Correlations between staining level of TRPs and the severity of dysmenorrhea, menstrual volume or uterus size. (A–C) Differences in TRPV1 (A), TRPM3 (B) or TRPA1 (C) expression among women with different degrees of dysmenorrhea severity. Spearman correlation coefficient and its statistical significance level are shown. (D and E) Correlations between TRPV1 (D), TRPM3 (E) or TRPA1 (F) staining level and menstrual volume. Spearman correlation coefficient and its statistical significance level are shown. (G–I) Scatter plot showing the relationship between uterine size (in mm³) and TRPV1 (G), TRPM3 (H) or TRPA1 (I) expression levels. Pearson's correlation coefficient, along with its statistical significance level, is also shown. The dashed line represents the regression line.

The Depth of Myometrial Infiltration Was Significantly Decreased After TRPM3 Inhibitor Primidone Treatment

The depth of myometrial infiltration of the ectopic endometrium was evaluated according to the criteria described by Bird.¹⁴ As shown in Figure 5D and E, compared with those in the control group, the mice in the ADE group exhibited significantly increased infiltration. After treatment with primidone for 3 weeks, the mice presented significantly less myometrial infiltration than the untreated mice. Although mice treated with atosiban displayed less myometrial infiltration than those in the ADE group, the difference was not significant ($P>0.05$).

Transcriptomic Analysis of the Uterine Tissue Following TRPM3 Inhibitor Primidone Treatment in a Mouse Adenomyosis Model

To identify the potential signaling pathway in which primidone is involved in addition to analgesic pathways, high-throughput RNA-seq was performed using uterine tissue from mice in the control, ADE model and primidone treatment groups ($n=3$). Compared with those in the control group, 517 genes were at least twofold differentially expressed in the tamoxifen-induced adenomyosis group: 271 were downregulated and 246 were upregulated. 133 genes, including 45 upregulated genes and 88 downregulated genes, were differentially expressed between the primidone treatment group and the ADE model group. Overall, 27 genes were upregulated in the ADE model group and then downregulated after primidone treatment, whereas 20 genes were downregulated in the ADE model group and then upregulated after primidone treatment. Hierarchical clustering analysis revealed systematic variation in the expression of mRNAs among these three groups (Figure 6A and B).

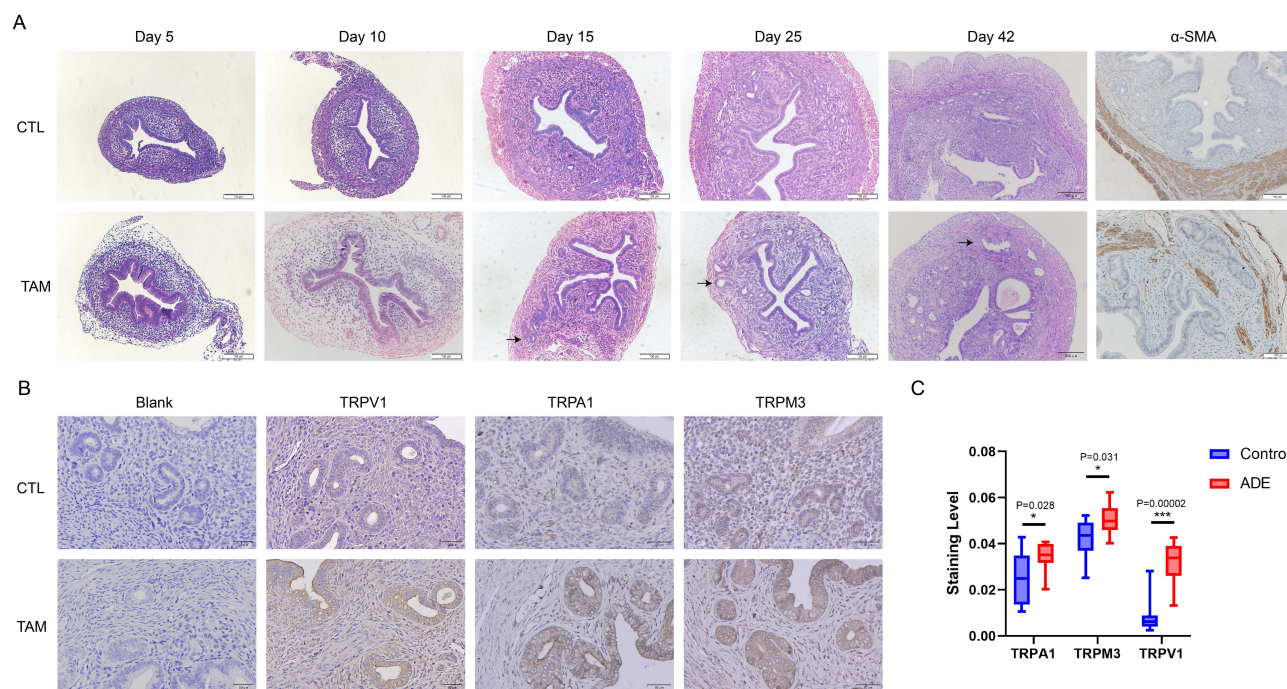


Figure 4 TRPV1, TRPM3 and TRPA1 expression in mice with tamoxifen-induced adenomyosis. **(A)** Representative images of HE staining at 5, 10, 15, 25 and 42 days of age and α -SMA immunostaining in mice with tamoxifen-induced adenomyosis (TAM) or those without (CTL) adenomyosis. The arrows indicate where the ectopic endometrium invaded the myometrium. **(B)** Representative images of TRPV1, TRPM3 and TRPA1 immunostaining in mice in the TAM and CTL groups at 42 days of age. Scale bars, 100 μ m. **(C)** Quantitative analysis via the two-tailed unpaired Student's *t*-test of TRPV1, TRPM3 and TRPA1 in mice of the TAM and CTL group at 42 days of age. Scale bars, 50 μ m. Symbols for statistical significance levels: **P* < 0.05 and ****P* < 0.001.

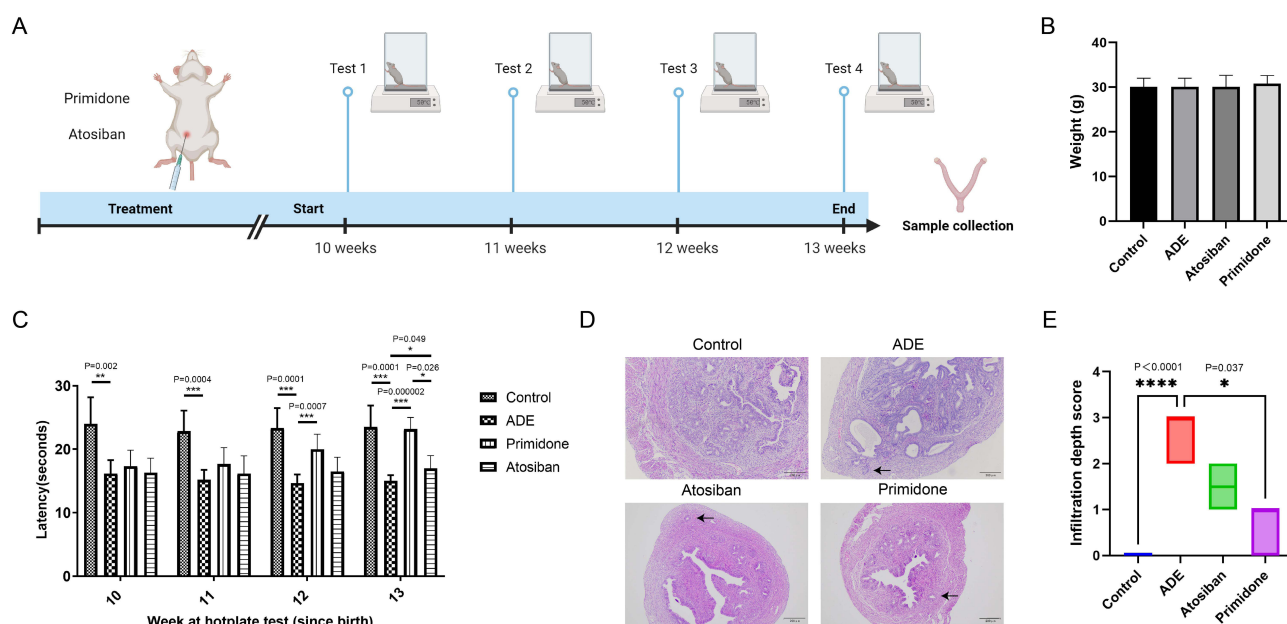


Figure 5 Primidone markedly prolonged the response latency and reduced myometrial infiltration in mice with tamoxifen-induced adenomyosis. **(A)** Diagram of the experimental timeline in mice, which was generated using BioRender.com. **(B)** Weights of the mice in the different treatment groups at 13 weeks of age. **(C)** Hotplate latency test results of mice subjected to primidone or atosiban treatment at the indicated times. **(D)** Representative images of HE staining in mice at 13 weeks of age after primidone or atosiban treatment. The arrows indicate where the ectopic endometrium invaded into the myometrium. Scale bars, 200 μ m. **(E)** Quantified grades of myometrial infiltration by the endometrium following treatment with primidone or atosiban in mice at 13 weeks of age. Symbols for statistical significance levels: **P* < 0.05, ***P* < 0.01, ****P* < 0.001 and *****P* < 0.0001.

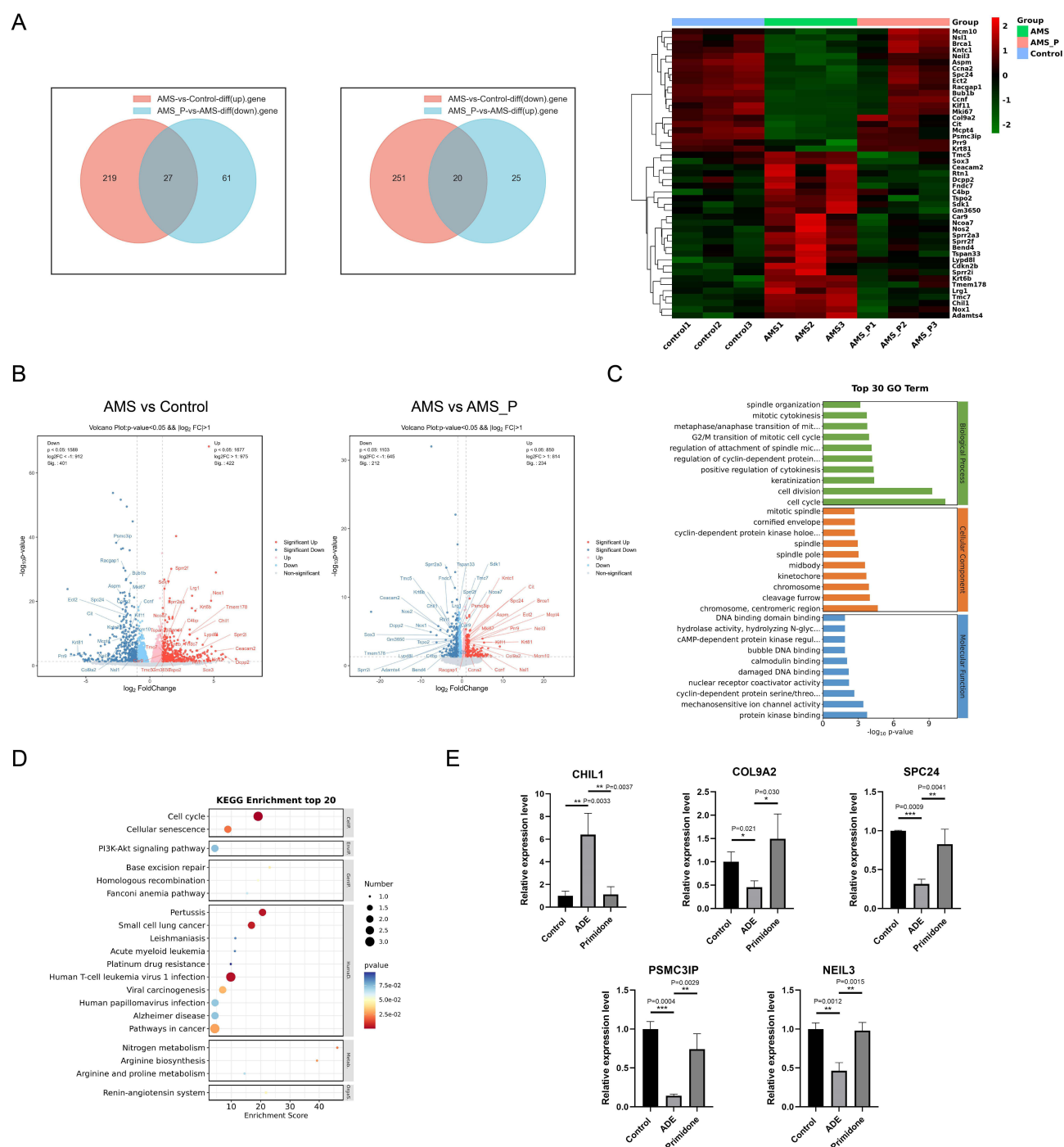


Figure 6 Analysis of transcriptome alternations in mouse uteri from control, adenomyosis model (AMS) and primidone treatment (AMS_P) groups. **(A)** Heatmap and Venn diagram of differentially expressed genes in uterus tissues from different groups. **(B)** Volcano plot of the RNAseq data from different groups. **(C)** The top 20 pathways enriched in the cell cycle and cell division. **(D)** Functional analysis of the DEGs in the uteri of mice from different groups. **(E)** Verification of CHIL1, COL9A2, PSMC3IP, NEIL3 and SPC24 gene expression by RT-PCR in the different groups. Symbols for statistical significance levels: * $P < 0.05$, ** $P < 0.01$ and *** $P < 0.001$.

The significantly enriched GO terms from the three groups were related mostly to the cell cycle and cell division (Figure 6C). GO terms related to chromosomes and the regulation of cytokinesis were also enriched. KEGG pathway enrichment analysis was also performed to determine the potential biological roles of the DEGs. The top 20 pathways with more than 2 DEGs were screened out, including “Cell cycle”, “Cellular senescence”, “Pathways in cancer”, and “PI3K-Akt signaling pathway”. Notably, more DEGs were associated with the “Cell cycle” than with any other pathway (Figure 6D).

Finally, we analyzed the expression of 5 genes by RT-PCR based on the fold changes in expression, as these genes were the top five DEGs screened in RNA-Seq and their prospective therapeutic value to verify our previous data. These genes were CHIL1, COL9A2, PSMC3IP, NEIL3 and SPC24. The expression ratios of these genes, as determined by RT-PCR, were consistent with those from the RNA-seq analysis (Figure 6E).

Discussion

Dysmenorrhea could be divided as primary and secondary dysmenorrhea according to its etiology. Primary dysmenorrhea occurs in the absence of pelvic pathology. It is mediated by elevated prostaglandin and leukotriene levels, with inflammation causing uterine contractility and cramping pain. Secondary dysmenorrhea is due to pelvic pathology or a recognized medical condition. Adenomyosis is the presence of endometrial glands and stroma within the myometrium, and is the most common cause of secondary dysmenorrhea.¹⁵ However, despite its common occurrence, it is underdiagnosed and undertreated. It has been reported that the disease is diagnosed on average 10 years after the onset of symptoms, and nonspecific complaints may lead to consultations regarding various medical management strategies.¹ Considering the significant effects of dysmenorrhea and other types of pain on women's reproductive health, further investigation is needed.

Pain can be divided into the following three categories: nociceptive pain, inflammatory pain and neuropathic pain. Dysmenorrhea and cyclic lower abdominal pain caused by ADE can initially be understood as nociceptive inflammatory pain.¹⁶ Interleukin-6, interleukin-8, TNF- α and PGE₂, which are considered proinflammatory factors, have been reported to be significantly increased in women with ADE.¹⁷ NSAIDs could well manage with pain caused by increasing level of prostaglandins through targeting COX enzymes. However, a review of 51 different clinical trials found that 18% of women reported minimal or no relief of menstrual pain with NSAIDs,⁵ which means that other pathways are likely involved in ADE-associated pain.

In recent years, primary disorders of the uterine layers with hyperperistalsis have been found to play an important role in pain mediator release and subsequent pain fiber activation.¹⁸ The increased frequency and magnitude of uterine contractions and neurotrophic factor secretion induced by the elevated OTR has been reported to contribute to the promotion of hyperinnervation and central sensitization, leading to dysmenorrhea and other types of pain in ADE patients.¹⁹ However, no research has been published on OTR inhibitors in either ADE patients or ADE animal models. Exercise²⁰ and nutritional interventions,²¹ such as supplementation or increased intake of omega-3 fatty acids and vitamin B, may also provide some benefit, but the evidence is limited to small randomized controlled trials (RCTs).

TRP channels are transmembrane protein complexes, and steroids, including estrogen, progesterone and androgens, have been found to affect the physiology of the cells and regulate where TRP channels are expressed.²² Regarding the roles of TRP channels in inflammatory pain, evidence suggests that inflammatory mediators can sensitize or alter the threshold of TRP channels, leading to pain behaviors.²³ Moreover, calcium is also a key player in a variety of important events, including fertilization, decidualization and implantation.²⁴ The functional expression of the calcium-conducting TRP channels TRPV2, TRPV4, TRPC6 and TRPM7 has been described in human endometrial stromal cells, and pregnancy outcomes in mice have been found to be perturbed by the deletion of TRPC6 channels,^{25,26} therefore, these channels are good candidates for intercellular signaling during processes such as decidualization and embryo implantation, in addition to pain control.

In our study, we first verified the mRNA expression of different subtypes of TRPV, TRPA, TRPM and TRPC channels by analyzing the eutopic endometrium of patients with and without adenomyosis. We found that except for TRPM2, TRPM5, TRPV1, TRPV2, TRPV3, TRPV6 and TRPC7, the expression of the other 14 TRP channels was increased significantly in the secretory phase in women without adenomyosis. These findings may support the hypothesis that they are regulated by ovarian hormones, which have been reported by other studies and their possible role in fertility.²⁴⁻²⁶ Until now, the causes of miscarriage are often unknown. However, in ~50% of early miscarriages the fetus exhibits chromosomal aberrations such as a structural alteration or abnormal chromosomal numbers. Several other factors have been associated with increased risk of miscarriage, such as parents' age, ethnic origin, psychological state of the mother, very low or very high pre-pregnancy BMI, feelings of stress, use of non-steroidal anti-inflammatory drugs, smoking and alcohol consumption have also been associated with significantly higher rates of miscarriage. Patients enrolled in this study were sporadic pregnancy loss and most of them did not receive chromosomal examination after miscarriage, therefore it's really hard to know the exact reason that leads to their miscarriages, which contribute to a limitation of the present study. Significantly

elevated expression of TRP channels other than TRPV4, TRPC7, TRPM2, TRPM4, TRPM5, and TRPM8 has been found in adenomyosis patients during the proliferative phase, suggesting their possible involvement in adenomyosis.

Next, we used IHC to determine the protein expression levels of TRPV1, TRPM3 and TRPA1, the most widely studied proteins in pain research, and found that TRPM3 and TRPA1 were significantly increased in the proliferative phase of patients with adenomyosis, which was consistent with the results at the mRNA level. Impressively increased expression of TRPV1 was exhibited in the secretory phase of the endometrium in adenomyosis patients versus the same phase of the endometrium in control patients, which may contribute to adenomyosis-related infertility. A close positive relationship between TRPM3 and the severity of dysmenorrhea was further determined by Spearman correlation analysis, suggesting its possible involvement in adenomyosis-associated pain. With the discovery of nociceptive TRP channels, pharmaceutical companies have expressed tremendous interest in TRP channels, as they hope to develop a new class of potent, safe analgesics. However, currently, the disadvantages of TRP channels have been most prominent. The activation or inhibition of a TRP channel may be beneficial for pain relief while simultaneously inducing unacceptable adverse effects. Indeed, the clinical development of TRPV1 antagonists has largely been halted because of hyperthermia,²⁷ while TRPA1-targeted drug development has encountered pharmaceutical and pharmacokinetic complications.²⁸ Therefore, the spotlight has recently moved to TRPM3.

Primidone and the flavone isosakuranetin have been reported as TRPM3 antagonists and are reassuringly devoid of serious side effects.^{29,30} Primidone is a medicine that has been used in clinics for epilepsy treatment. Recently, primidone has been reported to play an important role in thermal nociception attenuation through TRPM3 inhibition. Researchers are seeking its possible application in inflammation-related pain caused by a variety of diseases, such as acute pancreatitis³¹ and cystitis.³² Therefore, in the following experiment, we verified the possible effects of primidone on tamoxifen-induced adenomyosis in newborn ICR mice and compared them with those of atosiban, an oxytocin receptor antagonist. Although there are several ways to monitor spontaneous pain (such as writhing, abdominal squashing) and provoked pain (von Frey), adenomyosis-associated pain cannot be studied directly in mouse models, so general increased sensitivity to pain (hyperalgesia) is often used as a substitute measure, with the response time of mice to gradually increasing temperature indicating changes in central sensitization, so-called hotplate test. Though not ideal substitutes for analyzing adenomyosis-associated pelvic pain, such experiments are reasonable given the possible association between adenomyosis and neuropathic pain or sensory gain. Compared with that in mice from the control group, the hot plate response latency in mice from the ADE group was significantly decreased. TRPM3-deficient mice show inflammatory thermal hyperalgesia, pharmacological inhibition of TRPM3 may exert antinociceptive properties.²⁹ After 3 weeks of treatment with primidone, TRPM3 inhibitor, a significantly prolonged response latency was observed compared with the ADE group, indicating its antinociceptive effect in adenomyosis mouse model. In the future, the availability of primidone at therapeutic doses may be exploited to assess physiological and pathophysiological functions on human. Applying primidone at doses that are lower than those applied to treat convulsive disorders (<1.5g per day), the role of TRPM3 in mediating adenomyosis-related pain can be assessed. Finally, primidone may serve as a starting point for chemical modification to prevent a conversion to GABAA receptor-activating metabolites, and, thereby, to into a novel therapeutic target for adenomyosis with limited non-surgical treatment options.

As TRP channels are multifunctional signaling molecules with many roles in sensory perception and cellular physiology. Therefore, it is not surprising that TRP channels have been implicated in numerous diseases, including hereditary disorders caused by defects in genes encoding TRP channels (TRP channelopathies). Early drug discovery efforts to target TRP channels focused on pain, but as our knowledge of TRP channels and their role in health and disease has grown, these efforts have expanded into new clinical indications, ranging from respiratory disorders through neurological and psychiatric diseases to diabetes and cancer.²⁸ In our study, we found that primidone could also significantly decrease the depth of myometrial infiltration, which suggested that multiple pathological mechanisms may contribute to the effectiveness of TRPM3 inhibition. To clarify other possible mechanisms involved, transcriptomic analysis of mouse uteri from the control, ADE model and primidone treatment groups was performed. We first screened out the DEGs that were at least twofold differentially expressed and were increased/decreased in adenomyosis mice and then decreased/increased after primidone treatment. The DEGs were found to be the genes most strongly associated with “Cell cycle” and “Cell division” according to GO term enrichment and KEGG enrichment analyses, which reveals that these genes may be involved in the effectiveness of TRPM3 inhibition. Finally, based on the fold changes in expression

determined by RNA-Seq and their prospective therapeutic value, we verified the expression ratios of CHIL1, COL9A2, PSMC3IP, NEIL3, and SPC24. These genes play an important role in multiple pathological mechanisms, including inflammation, tissue remodeling, injury, DNA repair and cell mitosis, and thus these genes deserve further investigation.

CHIL1 belongs to glycoside hydrolase family 18, which is strongly associated with diseases such as asthma, arthritis, sepsis, diabetes, liver fibrosis, and coronary artery disease.³³ Moreover, following its initial identification in the culture supernatant of the MG63 osteosarcoma cell line, CHIL1 has been shown to be overexpressed in a wealth of both human cancers and animal tumor models.³⁴ Interestingly, CHI3L1-based targeted therapy has been increasingly applied to the treatment of tumors including glioma and colon cancer as well as rheumatoid arthritis.³³

PSMC3IP is a nuclear receptor coregulator involved in steroid hormone receptor-mediated transcription and a stimulator of DNA homologous recombination in DNA repair. Recently, the role of PSMC3IP is characterized in cancer development. PSMC3IP is upregulated in breast cancer. Inactivation mutation of PSMC3IP potentially contributes to an increased frequency of familial breast and ovarian cancer through regulating DNA repair.³⁵ In addition, decreased PSMC3IP and SPC24 have also been reported to contribute to female infertility via meiotic failure,^{36,37} which could be further studied in the field of adenomyosis-related reproductive issues.

NEIL3 is a versatile DNA glycosylase that repairs a diverse array of chemical modifications to DNA. Of 13 human cancers assessed from the Cancer Genome Atlas database, an increase in NEIL3 mRNA was recorded in all 13. In seven of the 13 cancers investigated, this overexpression of NEIL3 also correlated with increased somatic mutation load.³⁸ Besides, Patterns in NEIL3 expression and disease severity have been observed in age-dependent neurodegenerative disorders such as Alzheimer's disease (AD) and Parkinson's disease (PD).³⁹

Our study has two limitations. First, all ADE patients included in our study were the diffuse type. Due to the potentially different pathogenesis between diffuse and focal adenomyosis, it's uncertain if the results could be applied to focal adenomyosis. The presence of dysmenorrhea in the control group could be a bias, which might be mediated by elevated prostaglandin and leukotriene levels, with inflammation causing uterine contractility and cramping pain. Moreover, lack of a direct method for testing adenomyosis-associated pain in mouse models is a possible limitation of the present study. Second, the transcriptomic data in mice was obtained from whole uteri, which means that the differences we found might be due to diverse sources, such as endometrium (eutopic or ectopic) or myometrium. Further research would pinpoint the cells/areas affected using spatial transcriptomics to reveal the possible mechanisms of TRPM3 inhibitors like primidone in managing adenomyosis in different species, including human samples. Moreover, our research is only a preliminary step and does not reveal the full mechanism of TRPM3 antagonists. Genes that are shortlisted by this analysis should be investigated in vitro or in vivo models involving overexpression/knockdown studies, protein analyses and functional assays. We plan to perform these experiments in future studies.

Conclusion

In summary, we demonstrated that the expression of TRP channels varies significantly in adenomyosis patients throughout the menstrual cycle and that their expression is closely correlated with the severity of dysmenorrhea, metrorrhagia and uterus size. Moreover, primidone, a TRPM3 antagonist has been confirmed to have a significant effect on both the reduction of myometrial infiltration and analgesia in mice with tamoxifen-induced adenomyosis, which may provide a potential therapeutic option for adenomyosis treatment.

Abbreviations

ADE, Adenomyosis; NSAIDs, Non-steroidal anti-inflammatory drugs; TRPs, Transient receptor potential channels; TRPV, Transient receptor potential vanilloid; TRPA, Transient receptor potential ankyrin; TRPM, Transient receptor potential melastatin; TRPC, Transient receptor potential canonical; HE staining, Hematoxylin and eosin staining; RT-PCR, Real-time Polymerase chain reaction; IHC, Immunohistochemistry; ICR, Institute of Cancer Research; RNA-Seq, RNA sequencing; DEGs, Differentially expressed genes; SPSS, Statistical Package for the Social Sciences; OTR, Oxytocin receptor; RCTs, Randomized Controlled Trials.

Data Sharing Statement

The datasets used and/or analyzed during the present study are available from the corresponding author on reasonable request. The RNA-seq raw data was deposited in the Gene Expression Omnibus database (available: <https://www.ncbi.nlm.nih.gov/geo>; accession number GSE227384).

Ethics Approval and Consent to Participate

All experiments were performed under the guidelines of the National Research Council Guide for the Care and Use of Laboratory Animals. This study protocol was reviewed and approved by the Medical Ethics Committee of the First Affiliated Hospital of Soochow University (Suzhou, China), approval number 2020-149 and the Institutional Ethics Review Board of the Shanghai Obstetrics and Gynecology Hospital (Shanghai, China), approval number 2020-27. All tissue samples were obtained after written, full and informed consent from recruited subjects.

Acknowledgments

We are grateful to the women who participated in this study, OE Biotech Co. (Shanghai, China) for assisting in sequencing and/or bioinformatics analysis and Xishan Biotech Co. (Suzhou, China) for providing experimental platform.

Patient Consent for Publication

All patients involved in the research declare that they consent for publication of the manuscript.

Funding

The present study was supported by funding from the National Natural Science Foundation of China (No. 82001523 and No.82101215), Gusu Health Talent Project (No. GSWS2021004 and No.GSWS2023021) and the Jiangsu Province's "Shuang Chuang Tuan Dui".

Disclosure

The authors declare that they have no competing interests.

This paper has been uploaded to ResearchSquare as a preprint: <https://www.researchsquare.com/article/rs-3217639/v1>

References

- Borghese G, Doglioli M, Orsini B. et al. Progression of adenomyosis: rate and associated factors. *Int J Gynecol Obstet.* 2024;167(1):214–222. doi:10.1002/ijgo.15572
- Guo SW. Cracking the enigma of adenomyosis: an update on its pathogenesis and pathophysiology. *Reproduction.* 2022;164(5):R101–R121. doi:10.1530/REP-22-0224
- Di Donato N, Montanari G, Benfenati A, et al. Prevalence of adenomyosis in women undergoing surgery for endometriosis. *Eur J Obstet Gyn R B.* 2014;181:289–293.
- Vannuccini S, Luisi S, Tosti C, Sorbi F, Petraglia F. Role of medical therapy in the management of uterine adenomyosis. *Fertil Steril.* 2018;109(3):398–405. doi:10.1016/j.fertnstert.2018.01.013
- Oladosu FA, Tu FF, Hellman KM. Nonsteroidal anti-inflammatory drug resistance in dysmenorrhea: epidemiology, causes and treatment. *Am J Obstet Gynecol.* 2018;218(4):390–400. doi:10.1016/j.ajog.2017.08.108
- Takayama Y, Derouiche S, Maruyama K, Tominaga M. Emerging perspectives on pain management by modulation of TRP channels and ANO1. *Int J mol Sci.* 2019;20(14):3411. doi:10.3390/ijms20143411
- Samanta A, Hughes T, Moiseenkova-Bell VY. Transient Receptor Potential (TRP) channels. *Subcell Biochem.* 2018;87:141–165. doi:10.1007/978-981-10-7757-9_6
- Méndez-Reséndiz KA, Enciso-Pablo Ó, González-Ramírez R, Juárez-Contreras R, Rosenbaum T, Morales-Lázaro SL. Steroids and TRP channels: a close relationship. *Int J mol Sci.* 2020;21(11):3819. doi:10.3390/ijms21113819
- Duitama M, Moreno Y, Santander SP, et al. TRP channels as molecular targets to relieve cancer pain. *Biomolecules.* 2021;12(1):1. doi:10.3390/biom12010001
- Bamps D, Vriens J, de Hoon J, Voets T. TRP channel cooperation for nociception: therapeutic opportunities. *Ann Rev Pharmacol.* 2021;61:655–677. doi:10.1146/annurev-pharmtox-010919-023238
- Behrendt M. Transient receptor potential channels in the context of nociception and pain-recent insights into TRPM3 properties and function. *Biol Chem.* 2019;400(7):917–926. doi:10.1515/hsz-2018-0455
- Liu X, Nie J, Guo SW. Elevated immunoreactivity to tissue factor and its association with dysmenorrhea severity and the amount of menses in adenomyosis. *Hum Reprod.* 2011;26(2):337–345. doi:10.1093/humrep/deq311

13. Jin Z, Liu H, Xu C. Estrogen degrades Scribble in endometrial epithelial cells through E3 ubiquitin ligase HECW1 in the development of diffuse adenomyosis. *Biol Reprod.* **2020**;102(2):376–387. doi:10.1093/biolre/iox194
14. Bird CC, McElin TW, Manalo-Estrella P. The elusive adenomyosis of the uterus-revisited. *Am J Obstet Gynecol.* **1972**;112(5):583–593. doi:10.1016/0002-9378(72)90781-8
15. McKenna KA, Fogleman CD. Dysmenorrhea. *Am Fam Physician.* **2021**;104(2):164–170.
16. Gruber TM, Mechsner S. Pathogenesis of endometriosis: the origin of pain and subfertility. *Cells-Basel.* **2021**;10(6):1381.
17. Carrarelli P, Yen CF, Funghi L, et al. Expression of inflammatory and neurogenic mediators in adenomyosis. *Reprod Sci.* **2017**;24(3):369–375. doi:10.1177/1933719116657192
18. Agostinho L, Cruz R, Osório F, Alves J, Setúbal A, Guerra A. MRI for adenomyosis: a pictorial review. *Insights Imagine.* **2017**;8(6):549–556. doi:10.1007/s13244-017-0576-z
19. Zhang Y, Yu P, Sun F, Li TC, Cheng J, Duan H. Expression of oxytocin receptors in the uterine junctional zone in women with adenomyosis. *Acta Obstet Gyn Scan.* **2015**;94(4):412–418. doi:10.1111/aogs.12595
20. Azima S, Bakhshayesh HR, Kaviani M, Abbasnia K, Sayadi M. Comparison of the effect of massage therapy and isometric exercises on primary dysmenorrhea: a randomized controlled clinical trial. *J Pediatr Adol Gynec.* **2015**;28(6):486–491. doi:10.1016/j.jpag.2015.02.003
21. Pattanittum P, Kunyanone N, Brown J, Sangkomkhang US, Barnes J, Seyfoddin V. Dietary supplements for dysmenorrhoea. *Cochrane Db Syst Rev.* **2016**;3(3):D2124.
22. Uchida Y, Izumizaki M. Effect of menstrual cycle and female hormones on TRP and TREK channels in modifying thermosensitivity and physiological functions in women. *J Therm Biol.* **2021**;100:103029. doi:10.1016/j.jtherbio.2021.103029
23. Julius D. TRP channels and pain. *Annu Rev Cell Dev Bi.* **2013**;29:355–384.
24. Qu M, Lu P, Bellve K, Lifshitz LM, ZhuGe R. Mode switch of Ca²⁺ oscillation-mediated uterine peristalsis and associated embryo implantation impairments in mouse adenomyosis. *Front Physiol.* **2021**;12:744745. doi:10.3389/fphys.2021.744745
25. Hasna J, Abi NR, Sergeant F, Alfaidy N, Bouron A. The Deletion Of TRPC6 channels perturbs iron and zinc homeostasis and pregnancy outcome in mice. *Cell Physiol Biochem.* **2019**;52(3):455–467.
26. De Clercq K, Held K, Van Bree R, et al. Functional expression of transient receptor potential channels in human endometrial stromal cells during the luteal phase of the menstrual cycle. *Hum Reprod.* **2015**;30(6):1421–1436. doi:10.1093/humrep/dev068
27. Souza MDAD, Nassini R, Geppetti P, De Logu F. TRPA1 as a therapeutic target for nociceptive pain. *Expert Opin Ther Tar.* **2020**;24(10):997–1008.
28. Koivisto AP, Belvisi MG, Gaudet R, Szallasi A. Advances in TRP channel drug discovery: from target validation to clinical studies. *Nat Rev Drug Discov.* **2022**;21(1):41–59. doi:10.1038/s41573-021-00268-4
29. Krügel U, Straub I, Beckmann H, Schaefer M. Primidone inhibits TRPM3 and attenuates thermal nociception in vivo. *Pain.* **2017**;158(5):856–867. doi:10.1097/j.pain.0000000000000846
30. Straub I, Krügel U, Mohr F, et al. Flavanones that selectively inhibit TRPM3 attenuate thermal nociception in vivo. *Mol Pharmacol.* **2013**;84(5):736–750. doi:10.1124/mol.113.086843
31. Liu L, Liu H, Zhao M, et al. Functional upregulation of TRPM3 channels contributes to acute pancreatitis-associated pain and inflammation. *Inflammation.* **2024**.
32. Zhao M, Liu L, Chen Z, et al. Upregulation of transient receptor potential cation channel subfamily M member-3 in bladder afferents is involved in chronic pain in cyclophosphamide-induced cystitis. *Pain.* **2022**;163(11):2200–2212. doi:10.1097/j.pain.0000000000002616
33. Lee CG, Da SC, Dela CC, et al. Role of chitin and chitinase/chitinase-like proteins in inflammation, tissue remodeling, and injury. *Annu Rev Physiol.* **2011**;73:479–501. doi:10.1146/annurev-physiol-012110-142250
34. Libreros S, Garcia-Areas R, Shibata Y, Carrio R, Torroella-Kouri M, Iragavarapu-Charyulu V. Induction of proinflammatory mediators by CHI3L1 is reduced by chitin treatment: decreased tumor metastasis in a breast cancer model. *Int. J. Cancer.* **2012**;131(2):377–386. doi:10.1002/ijc.26379
35. Schubert S, Ripperger T, Rood M, et al. GT198 (PSMC3IP) germline variants in early-onset breast cancer patients from hereditary breast and ovarian cancer families. *Genes Cancer.* **2017**;8(1–2):472–483. doi:10.18632/genesandcancer.132
36. Biswas L, Tyc K, El YW, Morgan K, Xing J, Schindler K. Meiosis interrupted: the genetics of female infertility via meiotic failure. *Reproduction.* **2021**;161(2):R13–R35. doi:10.1530/REP-20-0422
37. Zhang T, Zhou Y, Wang HH, et al. Spc24 is required for meiotic kinetochore-microtubule attachment and production of euploid eggs. *Oncotarget.* **2016**;7(44):71987–71997. doi:10.18632/oncotarget.12453
38. Chen L, Huan X, Gao XD, et al. Biological functions of the DNA glycosylase NEIL3 and its role in disease progression including cancer. *Cancers.* **2022**;14(23):5722. doi:10.3390/cancers14235722
39. Oswalt LE, Eichman BF. NEIL3: a unique DNA glycosylase involved in interstrand DNA crosslink repair. *DNA Repair.* **2024**;139:103680. doi:10.1016/j.dnarep.2024.103680

Drug Design, Development and Therapy

Publish your work in this journal

Drug Design, Development and Therapy is an international, peer-reviewed open-access journal that spans the spectrum of drug design and development through to clinical applications. Clinical outcomes, patient safety, and programs for the development and effective, safe, and sustained use of medicines are a feature of the journal, which has also been accepted for indexing on PubMed Central. The manuscript management system is completely online and includes a very quick and fair peer-review system, which is all easy to use. Visit <http://www.dovepress.com/testimonials.php> to read real quotes from published authors.

Submit your manuscript here: <https://www.dovepress.com/drug-design-development-and-therapy-journal>

Dovepress
Taylor & Francis Group